Hindawi Publishing Corporation
Journal of Spectroscopy
Volume 2013, Article ID 217268, 13 pages
http://dx.doi.org/10.1155/2013/217268

Research Article

XPS Study of Mechanically Activated $YBa_2Cu_3O_{6+\delta}$ and $NdBa_2Cu_3O_{6+\delta}$

A. V. Fetisov,[1] G. A. Kozhina,[1] S. Kh. Estemirova,[1] V. B. Fetisov,[2] V. Ya. Mitrofanov,[1] S. A. Uporov,[1] and L. B. Vedmid'[1]

[1] *Institute of Metallurgy, Ural Branch of the Russian Academy of Sciences, 101 Amundsen Street, Ekaterinburg 620016, Russia*
[2] *Ural State Academy of Agriculture, Karl Liebknecht Street 42, Ekaterinburg 620075, Russia*

Correspondence should be addressed to G. A. Kozhina; gakozhina@yandex.ru

Received 27 February 2013; Accepted 30 March 2013

Academic Editor: Kong-Thon Tsen

Oxides $RBa_2Cu_3O_{6+\delta}$ (R=Y, Nd) subjected to mechanical activation in AGO-2 mill have been studied by X-ray photoelectron spectroscopy (XPS), thermal analysis, and magnetometry. It has been shown that mechanoactivation accelerates chemical degradation under the impact of H_2O and CO_2 in $YBa_2Cu_3O_{6+\delta}$ samples. Degradation occurs in the standard way. Investigation of mechanically activated $NdBa_2Cu_3O_{6+\delta}$ has revealed other results. It has been suggested that CO_2 can diffuse into its structure more freely than in $YBa_2Cu_3O_{6+\delta}$; as a result, carbonization may proceed directly in the volume of $NdBa_2Cu_3O_{6+\delta}$ and independently of the hydrolysis process. In addition, the mechanism of interaction between the oxide and water is not active and not "traditional" for the homologous series $REBa_2Cu_3O_{6+\delta}$ (where RE = rare earth and Y)—the characteristic "color" phase (Nd_2BaCuO_5) is not formed during hydrolysis. It is known that high-temperature treatment of $NdBa_2Cu_3O_{6+\delta}$ oxide results in partial substitution of cations Ba by Nd; which is accompanied by decrease in the superconducting transition temperature and formation of the impurity phase $Ba_2Cu_3O_{5+y}$. According to our data, mechanical activation of the resulting solid solution $Nd_{1+x}Ba_{2-x}Cu_3O_{6+\delta}$ unexpectedly has led to the reverse redistribution of cations, which has been manifested in the complete disappearance of the impurity phase and increase in T_c.

1. Introduction

Compounds $RBa_2Cu_3O_{6+\delta}$ (R=Y and Ln elements) are well known as high-temperature superconductors with the temperature of the transition to the superconducting state of 90–93 K [1]. The composition with R=Y is a standard material for superconducting electronics under development, cooled with liquid nitrogen [2, 3], the magnetic field sensor of π SQUID type [2], high current cables [4], and other products. Besides, this compound has very significant oxygen diffusion parameters, and there is an intention to use it as oxygen-ion conductor [5].

It is also known that the replacement of yttrium by neodymium results in the emergence of so-called "anomalous peak effect" [6], which leads to significant improvement of the superconducting transport properties of the material. An additional advantage of the oxide $NdBa_2Cu_3O_{6+\delta}$ (Nd-123) is its higher chemical stability by comparison with $YBa_2Cu_3O_{6+\delta}$ (Y-123) [7, 8]. The disadvantage of Nd-123 is ease of substitution of neodymium by barium ions in their structural positions during high temperature annealing [8–10], with the result that the temperature of the transition to the superconducting state (T_c) of the solid solution $Nd_{1+x}Ba_{2-x}Cu_3O_{6+\delta}$ appears to be relatively low and it decreases rapidly with increasing x (maximum T_c equal to 94 K was recorded at $x = 0$ [9], and $T_c \approx 80$ и 60 K were reported for $x = 0.08$ и 0.16, resp. [10]). Effect of substitution of barium by neodymium is amplified at high values of temperature and oxygen partial pressure [8, 9]. Simultaneously with the enrichment of the superconducting oxide by neodymium, to comply with cation balance in the system the impurity phase depleted in this element (e.g., $BaCuO_2$ [9]) is formed.

It should be noted that the superconducting properties of the solid solution $Nd_{1+x}Ba_{2-x}Cu_3O_{6+\delta}$ can be significantly reduced even when $x \to 0$ due to the mutual penetration

of Nd and Ba in the structural position of each other, which can occur during high-temperature annealing in an oxygen enriched atmosphere [9].

It is known [11] that high-intensity mechanical activation processing (hereinafter, MA) can significantly modify physicochemical properties of various materials. At the same time, such researches focused on the change of the functional properties of superconducting oxides $RBa_2Cu_3O_{6+\delta}$ (R-123) and to our knowledge have not yet been carried out (existing works like [12] are devoted to mechanical activation of precursors). Apparently this is related to the fact that the chemical stability of these oxides to the impact of air atmosphere components is not high even in the normal state [1]. Besides, mechanical treatment leads to substantial increase and activation of the free surface contacting with the atmosphere and during grinding spalling of R-123 particles occurs mainly along the basal plane of the crystallites and exposes the chemically active structural layer BaO [13]. Nevertheless, in the present study, we have attempted to assess how much the surface of R-123 actually degrades under MA and, just as importantly, what is the influence of this effect on the functional properties of these superconducting oxides. We have limited our investigations to compounds with R=Y, Nd, which are promising for applied developments.

Thus, the objectives of this work were (1) analysis of the chemical composition of the surface of mechanoactivated R-123 powders (hereinafter, MP) and determination of the degree of its chemical degradation under the influence of aggressive components of the environment: H_2O and CO_2; (2) analysis of the effect of mechanical activation on the functional properties of the superconducting material.

To fulfill the tasks we used the following methods: X-ray diffraction (XRD), thermal analysis, magnetometry, and X-ray photoelectron spectroscopy (XPS). The latter is a powerful tool to study the chemical and even phase composition of the material locally—in the thin layer (nearly 10 nm in thickness) of the external boundary. This method allows detecting impurity phases occurring at the average volume concentration outside the sensitivity of X-ray diffraction and also phases in the amorphous state.

2. Experimental Technique

Oxides R-123 were obtained by stepwise annealing a mixture of barium nitrate $Ba(NO_3)_2$ ("chemically pure" grade), the corresponding oxide of the rare earth element (RE), and basic copper carbonate $CuCO_3 \times Cu(OH)_2$ ("especially pure" grade) at 798 K for 5 h, 998 K (5 h), and 1213 K (140 h). The products were subjected to oxidative annealing by slow (with furnace) cooling from the synthesis temperature to 673 K and exposed to this temperature in air for 3 hours. The oxygen content of the samples $(6 + \delta)$ according to the oxidative annealing conditions can be estimated as 6.90 ± 0.03 [1]. The thus obtained material was "initial sample" (hereinafter, IP).

In the course of our research we also needed to obtain samples of Nd_2BaCuO_5 and Y_2BaCuO_5 to determine the spectral parameters of these compounds, as we did not find relevant and reliable data in the literature. They were synthesized at 1000°C for 23 h from previously obtained Nd-123 and Y-123 with the addition of necessary amounts of $BaCO_3$ and Nd_2O_3 (Y_2O_3). Before the synthesis homogenized mixtures of reagents were compressed into tablets.

Mechanical activation of the synthesized oxides Nd-123 and Y-123 was performed in a high energy AGO-2 planetary ball mill (set material: Fe) with acceleration of milling bodies of 60 g. The initial powders were dry milled for 0.5, 1, 2, and 10 min. The obtained materials were mechanically activated powders (hereinafter, MP), referred to, respectively, as N-0.5, N-1, N-2, N-10 (series of Nd-123) and Y-0.5, Y-2, Y-10 (series of Y-123). The particles size was determined using a scanning electron microscope Carl Zeiss EVO 40 (Germany) and amounted to $(3–5) \cdot 10^{-6}$ m, while the particles themselves were agglomerates consisting of stuck together crystallites with the size of nearly $0.3 \cdot 10^{-6}$ m.

X-ray examination of samples was carried out using a diffractometer Shimadzu XRD-7000 (Japan). The size of coherent scattering regions (CSR) was determined by X-ray diffraction analysis using the approximation method [14]. Silicon powder was used to determine the instrumental broadening of the diffraction lines. Selection of the function for approximating diffraction peaks was made using the program [15].

Thermal studies were carried out using the thermal analyzer Netzsch STA 449C Jupiter (Germany), combined with a mass spectrometer Netzsch QMS 403C Aëolos (Germany) for evolved gas analysis. The rates of heating and cooling of samples were 10 K/min.

The magnetization (m) was measured using a commercial vibrating sample magnetometer Cryogenic CFS-9T-CVTI in the temperature range 4.2–300 K. The measurements in the heating mode were performed on samples cooled in a magnetic field (field cooling, FC) and in the absence of magnetic field (zero field cooling, ZFC).

XPS study was performed on a Omicron Multiprob spectrometer (Germany). The test sample ($RBa_2Cu_3O_{6+\delta}$ powder and R_2BaCuO_5 ceramic tablet, where R=Y, Nd) was attached to the sample holder using conductive double-sided adhesive tape and moved into the workspace of the spectrometer. Ceramic samples were subjected to scribing in ultrahigh vacuum before study. The source of the exciting radiation for XPS was Mg-anode of X-ray gun with 170 W. The energy scale of the spectrometer was calibrated by the binding energies of the peaks: Au $4f_{7/2}$ (84.00 eV), Ag $3d_{5/2}$ (368.29 eV), and Cu $2p_{3/2}$ (932.67 eV). The value of samples surface charge was determined by the difference between the measured binding energy of the C 1s signal due to C–H groups and the value of 285.0 eV. Wide-scan survey spectra were recorded with 0.5 eV energy step and the signal accumulation time of 1 s at the pass energy (E_{PE}) of 100 eV. High-resolution spectrum was recorded with 0.05 eV energy step, exposure time of 7.5 s (15 scans by 0.5 s), and $E_{PE} = 20$ eV. The accuracy of peak position determination in the latter case was 0.1 eV. Decomposition of the spectra into components and extraction of the background were performed by the Shirley method using the program XPSPeak 4.1.

3. Experimental Results

3.1. Oxides Y_2BaCuO_5 and Nd_2BaCuO_5

Attestation of Y_2BaCuO_5 and Nd_2BaCuO_5 Oxides by XRD and XPS Methods. X-ray analysis has not shown the presence of any impurity phases in the synthesized oxides Y_2BaCuO_5 and Nd_2BaCuO_5. Syngony, space group, and lattice parameters for Y_2BaCuO_5 oxide are, respectively, orthorhombic, Pbnm, a = 7.1304(6) Å, b = 12.1761(10) Å, c = 5.6571(6) Å, for Nd_2BaCuO_5 oxide: tetragonal, P4/mbm, a = 6.6950(5) Å, c = 5.8188(9) Å.

The results of XPS study of these oxides are shown in Figure 1. Decomposition of the obtained electronic spectra was carried out on the basis of choosing the most appropriate model for the phase composition of the surface and the mutual coherence between the spectra of different elements (with adjustments taking into account the analyzer transmission efficiency and differences in the photoionization cross-section). The spectrometric data for oxides BaO, Y_2O_3, Nd_2O_3, and barium carbonate were taken from [16, 33–35], respectively.

Let us discuss some controversial points arising during decomposition of the spectra. As can be seen from Figure 1, in the spectra of the sample containing neodymium, there are the intense peaks at 779.0 (Ba $3d_{5/2}$) and 528.6 (O 1s) eV, which coincide with the signal from BaO [33] with high accuracy. This can mean that the synthesis of the sample has not been completed, and the unspent furnace charge components have been localized in the surface layer of the material (location explains the fact that X-ray analysis, unlike XPS, has not revealed the presence of impurity oxides in the sample), hiding the main compound (Nd_2BaCuO_5) and making its identification ambiguous. To test this hypothesis, we have prepared one more sample Nd_2BaCuO_5 at more high the synthesis temperature—1050°C. It was expected that if indicated signals belonged to BaO, their intensity would significantly decrease along with increase in intensity of the main compound peaks after the new heat treatment. But nothing like this has happened—the intensity of all the peaks stayed the same. That proves that the peaks at 779.0 (Ba $3d_{5/2}$) and 528.6 (O 1s) eV relate directly to the oxide Nd_2BaCuO_5.

In addition to the main compound, there is a barium carbonate on the surface of Nd_2BaCuO_5 sample; that is confirmed by the peak of corresponding intensity at 289.1 eV in the spectrum of C 1s; see Figure 1. This presence is apparently due to insufficiently complete decomposition of source $BaCO_3$ involved in the synthesis, (there was not barium carbonate on the surface of the sample synthesized at 1050°C; however, there was a similar amount of unidentified barium compound with the binding energy of Ba $3d_{5/2}$ electronic level of 780.7 eV).

Next we turn our attention to the sample Y_2BaCuO_5, for which the intensity of the barium oxide peak in O 1s spectrum, according to calculations, should be negligible and amount to ~1/50 of the main compound peak intensity. However, in a given location of the spectrum (more precisely, near 529 eV) there is a clear peak, whose intensity is about 1/4 of the intensity of the peak that is near (referred to Y_2BaCuO_5 compound). We suppose that this small peak also belongs to the main compound. Indeed, O 1s peak of Y_2BaCuO_5 at 531.3 eV is located near the corresponding peak of the yttrium oxide (see Figure 1), which is explained by the presence of the same type of Y–O bond in both oxides. Meanwhile, there is also a Ba–O bond in Y_2BaCuO_5 compound, which should be reflected by additional oxygen peak located near the O 1s-peak of barium oxide. Note that only one peak was enough to describe O 1s spectrum of Nd_2BaCuO_5.

Quantitative analysis of the elements, carried out on the basis of the decomposition of the spectra, has shown a good agreement with formula composition for both compounds under study.

3.2. Oxides $YBa_2Cu_3O_{6+\delta}$ and $NdBa_2Cu_3O_{6+\delta}$

3.2.1. X-Ray Diffraction Study of Oxides $YBa_2Cu_3O_{6+\delta}$ and $NdBa_2Cu_3O_{6+\delta}$. The obtained lattice parameters data and the size of the coherent scattering region are presented in Table 1. One can see that the first 1-2 minutes of grinding lead to a significant decrease in the size of CSR in both superconductors, that is, refinement of the microstructure. With increasing milling duration up to 10 min further changes of CSR-size practically do not occur. However, there is a fundamental difference in the effect of mechanical activation on the phase composition of Y-123 and Nd-123. In the initially single-phase yttrium superconductor with increasing milling duration, the amount of impurity phase (Y_2BaCuO_5) increases continuously, whereas in the neodymium superconductor it is vice versa—a small amount of impurity phase ($Ba_2Cu_3O_{5+x}$) existing in the initial sample is not observed in all mechanically activated samples. This confirms the findings of the high chemical stability of Nd-123 oxide by comparison with its yttrium homologue.

Another interesting point worthy of discussion is the fact that there is no more than one impurity in all the tested samples (Y-123 and Nd-123); that, according to the mass balance, should affect the cation stoichiometry in the main phase of the sample.

As for Nd-123 samples, deviations from the ideal cation stoichiometry after a long (150 hours) high-temperature annealing is just a characteristic feature of them [9]. Appearance of impurity $Ba_2Cu_3O_{5+x}$ phase in an amount of 3% indicates that the IP of Nd-123 (sample N-0) is in fact a solid solution $Nd_{1.03}Ba_{1.97}Cu_3O_{6+\delta}$. Unspent Ba (in amount of ~3%) seems to form under atmospheric moist air the X-ray amorphous phase of $Ba(OH)_2 \cdot nH_2O$, which is easily transformed into $BaCO_3$ from the surface due to the presence of CO_2 in the air.

Y-123 MP, which contains a rich by yttrium impurity Y_2BaCuO_5, to comply with the ion balance, should include the phase not containing this element. Since these phases were not detected by XRD, we have assumed that as a result of mechanical activation they became X-ray amorphous. In fact, they were later identified by us with the use of XPS; see later.

3.2.2. XPS Study of $YBa_2Cu_3O_{6+\delta}$ Oxide. Figure 2 shows the survey spectra of the powders $YBa_2Cu_3O_{6+\delta}$ under study.

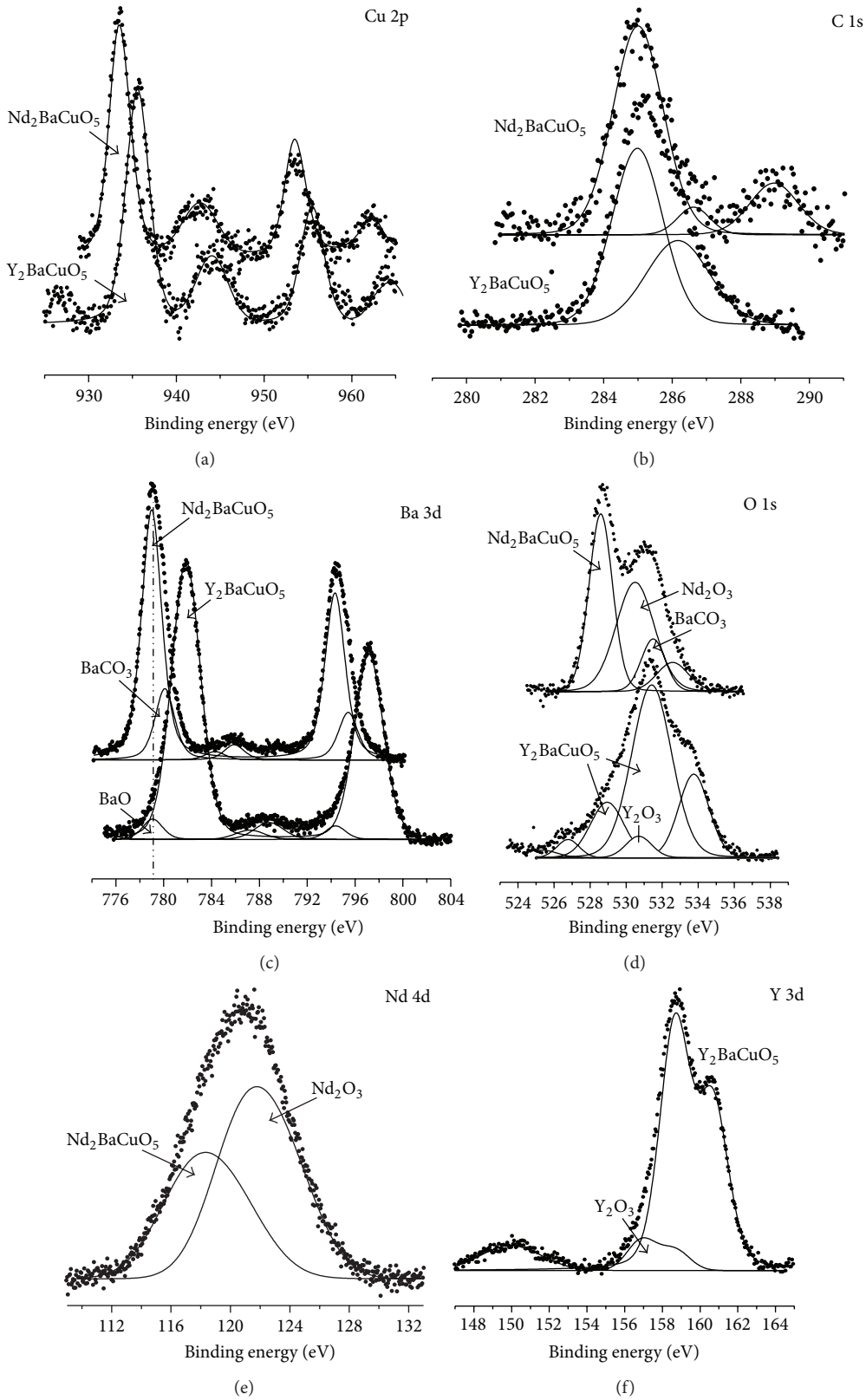

Figure 1: XPS spectra of Y_2BaCuO_5 and Nd_2BaCuO_5 oxides. The peaks related to the main oxide are marked by bold lines. The ordinate hereinafter is the intensity of the XPS signal in arbitrary units. To reduce the figure size, the *y*-axis itself is not shown.

Table 1: Phase composition, lattice parameters, and the size of coherent scattering regions (L) for $YBa_2Cu_3O_{6+\delta}$ and $NdBa_2Cu_3O_{6+\delta}$ before and after mechanical treatment.

Crystallographic parameters	Milling duration in AGO-2			
	(1) $YBa_2Cu_3O_{6+\delta}$ powders			
	0 s (sample Y-0)	30 s (sample Y-0.5)	2 min (sample Y-2)	10 min (sample Y-10)
The main phase—orthorhombic S.G. Pmmm				
a, Å	3.8208(3)	3.8218(3)	3.8287(10)	3.8344(10)
b, Å	3.8884(5)	3.8893(5)	3.8938(15)	3.8879(15)
c, Å	11.6809(11)	11.6793(12)	11.6739(33)	11.6663(31)
V, Å^3	173.541(53)	173.599(55)	174.036(161)	173.919(158)
Impurity, mass%	—	~5% Y_2BaCuO_5	~5% Y_2BaCuO_5	~7% Y_2BaCuO_5
L, nm	167	57	25	20
	(2) $NdBa_2Cu_3O_{6+\delta}$ powders			
	0 s (sample N-0)	30 s (sample N-0.5)	2 min (sample N-2)	10 min (sample N-10)
The main phase—orthorhombic S.G. Pmmm				
a, Å	3.8677(1)	3.8731(3)	3.8727(12)	3.8754(12)
b, Å	3.9202(1)	3.9206(10)	3.9225(14)	3.9161(15)
c, Å	11.7612(3)	11.7622(24)	11.7630(39)	11.7661(24)
V, Å^3	178.328(6)	178.608(118)	178.688(178)	178.564(212)
Impurity, mass%	~3% $Ba_2Cu_3O_{5+x}$	—	—	—
L, HM	179.2	32.5	22.9	16.9

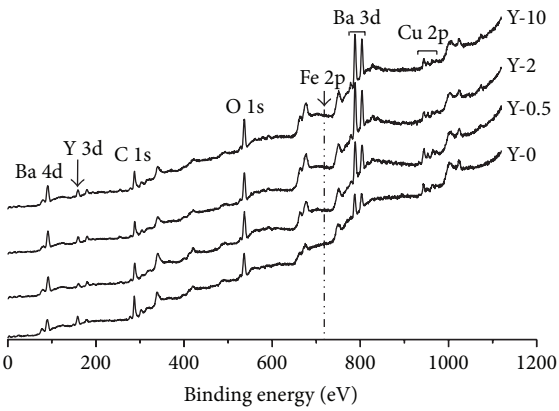

Figure 2: XPS survey spectra of the initial and mechanoactivated $YBa_2Cu_3O_{6+\delta}$ samples.

Recording such spectra conducted in high sensitivity mode (at high E_{PE}) allows to consider the main lines of all elements presented in the surface layer of the material in amounts greater than 0.3 at.%. As could be expected, there are peaks of the electronic levels of yttrium, barium, copper, and oxygen contained in the composition of the oxide under study. The C 1s peak includes a signal from the carbon contamination of the random nature.

One can see (Figure 2) that on the surface of MP samples there is no iron (mill headsets material), leading to the appearance of specific magnetic and superconducting properties of the material. Strongly increased barium peak (represented as a doublet of Ba $3d_{5/2}$–Ba $3d_{3/2}$) in the spectra of activated samples testifies the redistribution of elements between the volume and surface occurs, which is usually the result of chemical degradation of the surface under the influence of an environment. In this case, it could be a well-established [36] reactions as follows:

$$2YBa_2Cu_3O_{6.5+x} + 3H_2O \longrightarrow Y_2BaCuO_5 + 3Ba(OH)_2 + 5CuO + \uparrow xO_2, \quad (1)$$

$$Ba(OH)_2 + CO_2 \longrightarrow BaCO_3 + H_2O. \quad (2)$$

Table 2 summarizes the obtained $BaCO_3$ of CP grade, calcinated at 700°C, Y_2BaCuO_5 and taken from the literature of spectrometric data for the reactants involved in the reactions (1) and (2) for reliable identification of the peaks of these compounds in the spectra of the samples under study.

High-resolution XPS spectra showing the characteristic electronic levels of the elements constituting Y-123 samples are presented in Figure 3.

The analysis of the Ba 3d spectra has showed that in addition to barium carbonate (line Ba $3d_{5/2}$ at 779.9 eV) there is the phase Y_2BaCuO_5 (line Ba $3d_{5/2}$ at ~782 eV) on the surface of the samples. The line Ba $3d_{5/2}$ at 778.0 eV, which is observed only in the IP, is directly owned by Y-123 (see Table 2). The Y 3d spectra confirm the presence of Y_2BaCuO_5-phase on the surface of samples; the substance's line Y $3d_{5/2}$ at 158.7 eV is clearly visible in these spectra (see Table 2). Besides, the Y 3d spectra reveal the surface contains the following oxides: Y_2O_3 [34] (line Y $3d_{5/2}$ at 156.9 eV), Y-123

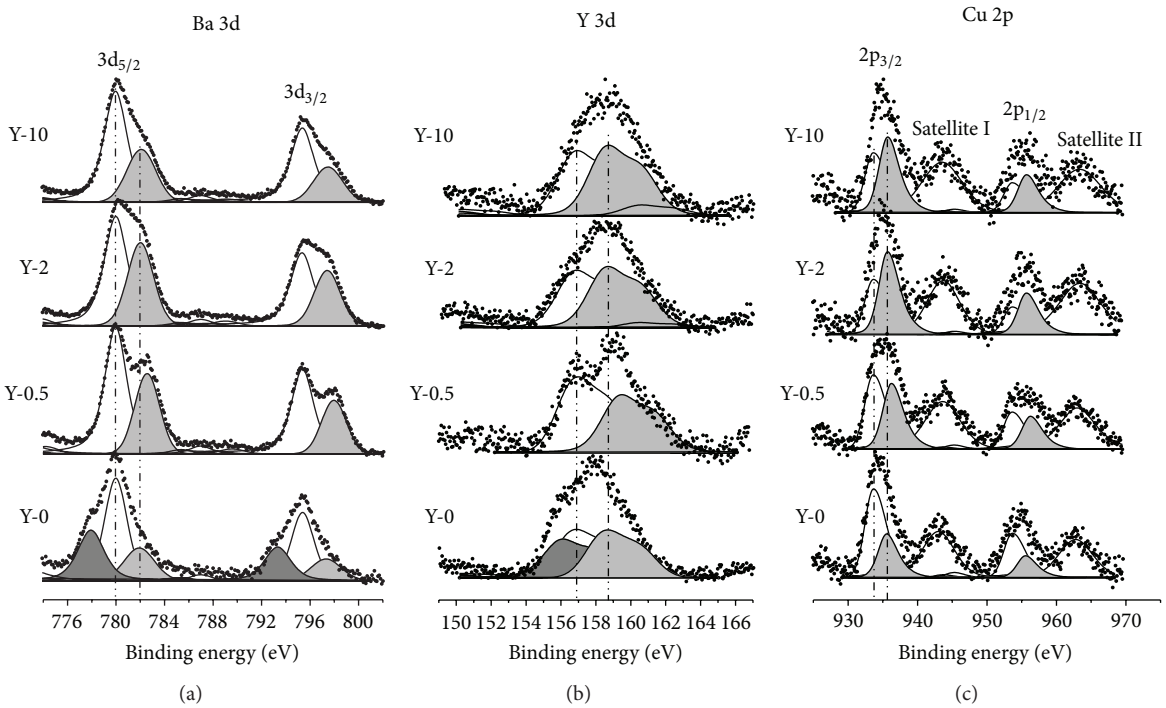

Figure 3: XPS spectra of $YBa_2Cu_3O_{6+\delta}$ powders. Dark shading: the main phase signal; light shading: Y_2BaCuO_5 signal.

Table 2: The positions of the characteristic XPS lines of barium compounds.

Electron orbital	$BaCO_3$	$Ba(OH)_2$	Y-123	Y_2BaCuO_5
		Binding energy, eV		
Ba $3d_{5/2}$	779.9 [16, 17] 779.8*	781.3 ± 0.1 [18, 19]	777.7 ± 0.1 [20–23]	781.9*
Ba $4d_{5/2}$	89.3*		87.5 [22]	
Y $3d_{5/2}$			156.0 ± 0.2 [21, 24, 25]	158.7*
Cu $2p_{3/2}$			933.5 [21, 26]	935.6*
O 1s	531.4 ± 0.1 [16, 17] 531.4*	531.2 эВ [27]	528.45 ± 0.05 эВ [20–23]	(529.1, 531.3)*
C 1s	289.25 ± 0.15 эВ [16, 17] 289.4*			

*Our data.

(line Y $3d_{5/2}$ at 156.0 eV in the spectrum of IP) and the phase $Y_2(C_2O_4)_3$ [37] (line Y $3d_{5/2}$ at 160.1 eV). The presence of Y_2BaCuO_5 compound in samples is also reflected in the spectra of Cu 2p: a high-energy doublet (main peak at 935.6 eV) corresponds to it. At the same time, the low-energy Cu 2p-doublet parameters are close to those found in [22] for Y-123: the main peak at 933.5 eV, a satellite at ~943 eV, as well as parameters relating to copper oxide Cu (II) [28]: 933.6 eV and 942.5 eV, respectively. However, from the analysis of the spectra of Ba 3d and Y 3d (see earlier), it can be argued that the Cu 2p signal from the phase of Y-123 may be only in the spectrum of IP samples.

Thus, in addition to the main phase, the surface of IP contains the final products of the reactions (1) + (2) and Y_2O_3 phase probably sourced by the initial precursor incompletely consumed during the synthesis of $YBa_2Cu_3O_{6+\delta}$. As a result of MA treatment, the surface of the powder is covered with a layer of yttrium oxide and the products of reactions (1) + (2) to a considerable depth of at least 10 nm (judging by the amount of Y_2BaCuO_5 phase in the samples determined by XRD).

3.2.3. XPS Study of $NdBa_2Cu_3O_{6+\delta}$ Oxide. Figure 4 demonstrates the survey spectra of Nd-123 powders. One can see that, as in the case of Y-123 samples, the signal representing the iron was not observed for any intensive milling duration. The feature of Nd-123 samples is rather low intensity of the Ba 3d and Ba 4d peaks for powders activated for 0.5 and 2 min (compare Figure 4 with Figure 2 for Y-123 powder). Barium peaks has markedly increased (as well as oxygen O 1s peak) only at 10 min of activation.

Figure 5 shows the high-resolution spectra of the electronic levels of barium (3d and 4d), neodymium (4d), and copper (2p) in powders with different activation prehistory. In the barium spectra the high-intensity peaks at 779.9 eV ($3d_{5/2}$) and 89.3 eV ($4d_{5/2}$) are obviously responsible for the compound $BaCO_3$, and the low-intensity peaks at 778.0 and 87.6 eV, which are observed only in IP samples (dark shaded in Figure 5), correspond to the main phase by analogy with Y-123 samples. The analysis of Cu 2p spectra has revealed the presence of copper ions with the electronic structure similar to that in Y-123 or in CuO oxide.

However, as seen in Figure 5, the state Cu 2p with high binding energy (935.9 ± 0.3 eV) is also present in all Nd-123 samples. According to our data (see Table 3), this state is not typical for simple and ternary compounds of copper. During MA processing, its share in Cu 2p spectra changes in strict accordance with the high energy components of the Ba 3d and Ba 4d spectra, light shaded in Figure 5 (at 781.7 eV (Ba $3d_{5/3}$) and 91.9 ± 0.3 eV (Ba $4d_{5/3}$)), which implies that a double oxide of barium-copper was on the surface of the samples. We tend to identify this oxide as $Ba_2Cu_3O_{5+x}$ phase, which was detected by X-ray diffraction analysis of IP samples (see Table 1). Despite the fact that this phase was not found by XRD in samples N-0.5, N-1, and N-2, it is visible in the XPS spectra due to the effect of spatial localization.

According to Figure 5, the surface of the samples also contained the oxide Nd_2O_3 (line Nd $4d_{5/2}$ at 121.1 eV), which under intense grinding, at the initial stages, was partly transformed into $Nd_2(C_2O_4)_3$ [37] (line Nd $4d_{5/2}$ at ~122.5 eV). Based on the analysis of possible superpositions of the spectra of Ba 3d, Ba 4d, and Cu 2p, the low-energy Nd 4d doublet (line Nd $4d_{5/2}$ at 115.7 eV), the intensity of which is almost independent of the MA duration, belongs to a double oxide $NdCu_yO_{1.5+y+z}$ of undetermined composition. The Nd 4d doublet of the main compound, apparently, overlaps with one of the previously noted signals, and so it is shown explicitly in Figure 5.

On the intensity ratios of the peaks in Figure 5, one can construct a model of the relative position of the phases Nd-123, $BaCO_3$, and $Ba_2Cu_3O_{5+x}$ in the surface layer of the material (this method has been used, e.g., in [22] to analyze the relative position of the layers Y-123 and $BaCuO_2$). To realize this we use the dependence of the layer thickness, analyzed by XPS (usually taken as $3 \cdot \lambda_m$), on the kinetic energy of the electrons [38], referring to the electrons, giving the corresponding lines in the spectra of Ba 3d and Ba 4d as follows:

$$\lambda_m = 2170E_k^{-2} + 0.72(aE_k)^{1/2}, \quad (3)$$

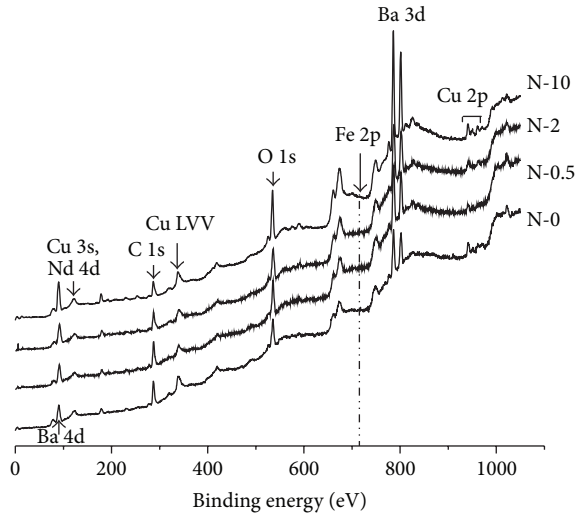

Figure 4: XPS survey spectra of the initial and mechanoactivated $NdBa_2Cu_3O_{6+\delta}$ samples.

where λ_m is the electron mean free path, expressed in monolayers, a is monolayer thickness in nm, E_k is kinetic energy in eV ($E_k = h\nu - E_{BE} - \varphi$), $h\nu = 1253.6$ eV is the energy of the exciting radiation, used in XPS analysis, E_{BE} is the binding energy of the electronic level under analysis, and φ is the work function of the spectrometer (3.46 eV).

According to this relationship, the thickness of the layer under analysis increases monotonically with increasing E_k in the range $E_k > 40$ eV. As can be seen from Figure 6, increase in the thickness of the layer under analysis can affect the following volume ratios detectable by XPS: phase I/phase III, and phase II/phase III and has no influence on the volume relation: phase I/phase II. The phase fraction to a first approximation is proportional to the area under corresponding XPS peak. Therefore, based on the ratio of areas of the different lines in the spectra in Figure 5, one can conclude that both barium-containing products of chemical decomposition of Nd-123 are located atop of the main oxide, that is, correspond to phases I and II in Figure 6. The thickness of the degraded layer in N-10 sample is ~10 nm (as the original phase is barely visible through it) and in IP (N-0) sample it is estimated to be 5-6 nm.

It should be noted, however, that such a small thickness of $Ba_2Cu_3O_{5+x}$ layer in IP has not prevented this phase to be recognized by XRD analysis (see Table 1). One can therefore conclude that IP particles contain, in addition, a considerable amount of $Ba_2Cu_3O_{5+x}$ in the form of individual inclusions in bulk (as a result of this oxide synthesis features; see Section 1). During MA processing, material particles cracked and inclusions went outside, resulting in the fraction of $Ba_2Cu_3O_{5+x}$ phase on the surface increased up to a point (up to 1 min, inclusive). The subsequent decrease in this phase (see Figure 5) is apparently due to the fact that another process also developed on the surface during grinding: spending of $Ba_2Cu_3O_{5+x}$ involving the original solid solution $Nd_{1+x}Ba_{2-x}Cu_3O_{6+\delta}$ to formation of cation-stoichiometric $NdBa_2Cu_3O_{6+\delta}$. To prove the occurrence of such interaction,

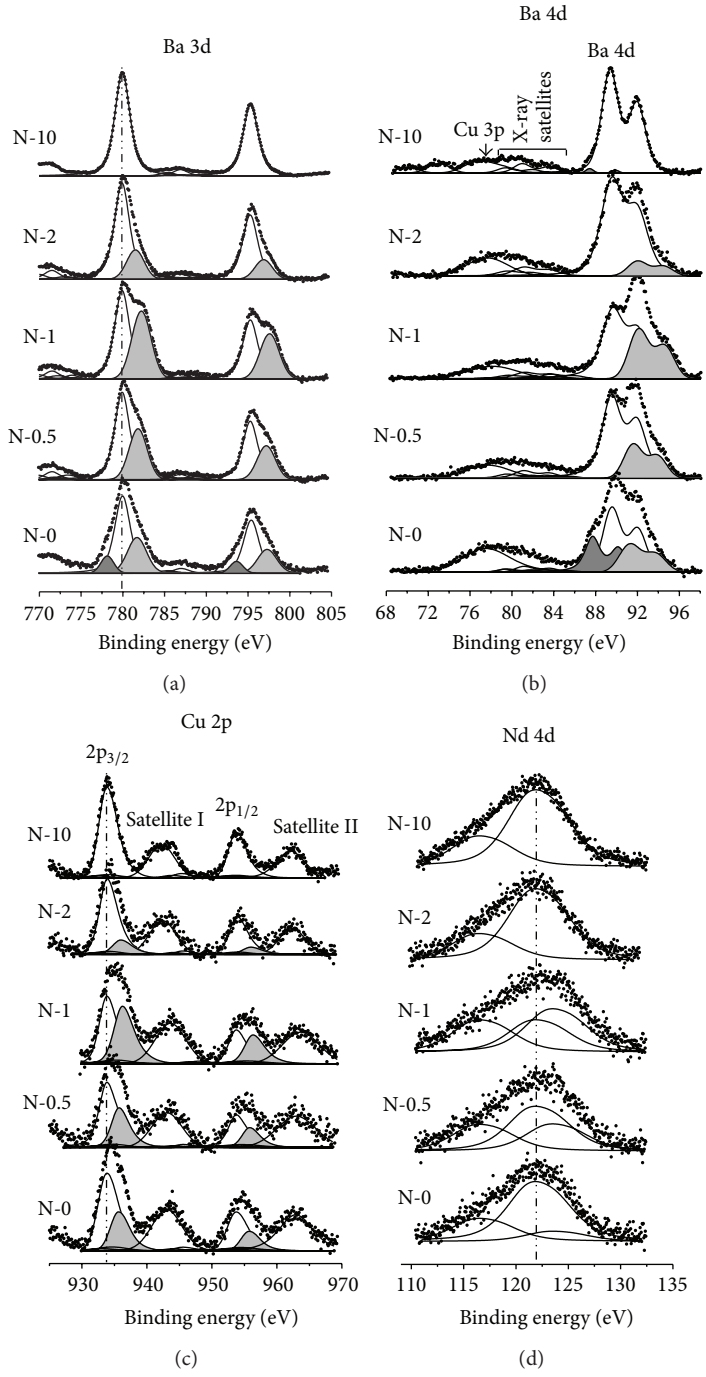

Figure 5: XPS spectra of $NdBa_2Cu_3O_{6+\delta}$ powders.

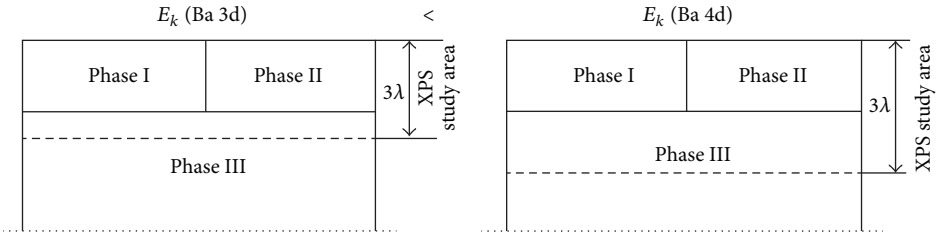

Figure 6: Analysis of the mutual arrangement phases in the surface layer of the material and their volume relations from XPS data.

Table 3: Characteristic spectral parameters of different copper compounds.

Electron orbital	CuO	$CuCO_3$	$Cu(OH)_2$	$Cu_2CO_3(OH)_2$	Nd_2BaCuO_5
			Binding energy, eV		
Ba $3d_{5/2}$					779.0*
Nd $4d_{5/2}$					118.2*
Cu $2p_{3/2}$	933.7 ± 1 [28–30]	934.8 [28]	934.74 ± 0.06 [29, 31]	934.7 [32]	933.5*
O 1s	529.74 ± 0.06 [30, 31]		531.24 [31]		528.6*

*Our data.

later we present the data of magnetic measurements, which indicate that MA treatment results in significant increase in the temperature of the superconducting transition in separate regions of the material.

3.2.4. Thermal Analysis of $YBa_2Cu_3O_{6+\delta}$ and $NdBa_2Cu_3O_{6+\delta}$. Samples of R-123 have been studied by thermogravimetry coupled with mass-spectrometry to analyze the gases evolved during experiments. Results of the study are summarized in Figure 7. It is seen that reversible change in mass of IP-samples occurs in the range of 430–900°C; that must be due to oxygen exchange between nonstoichiometric R-123 oxides and the gas phase taking place at these temperatures [1]. MP samples start losing mass sharply around 70°C when heated. Mass spectrometry analysis of thermal desorption products indicates the presence of large amount of water and a small amount of carbon dioxide contained in the samples in the form of $BaCO_3$ (the temperature range in which the CO_2 was released and the value of p_{CO_2} used for thermal analysis of the atmosphere was consistent with conditions of barium carbonate decomposition).

3.2.5. Study of Magnetic Properties of $YBa_2Cu_3O_{6+\delta}$ and $NdBa_2Cu_3O_{6+\delta}$. Temperature dependences of ZFC magnetization of the samples Y-0, Y-0.5, Y-2, and Y-10 are shown in Figure 8. A sharp downturn in magnetization at ~90 K observed in the samples Y-0, Y-0.5, and Y-2 clearly shows the presence of the superconducting phase. Superconducting transition temperatures of the samples Y-0, Y-0.5, and Y-2 have been determined by taking the derivative of the magnetization against the temperature (dm/dT). Thus, defined temperatures T_c are equal to 91 K for the samples Y-0 and Y-0.5 and 88 K for the sample Y-2. A wide transition width around T_c = 90 K indicates that both the initial and MP samples contain inhomogeneous superconductor phases with different T_c. The following facts indicate the presence of paramagnetic contribution in the magnetization behavior of MP samples and its growth with increasing milling duration: a significant increase in magnetization m of the samples Y-0.5 and Y-2 compared with the initial sample Y-0 at the temperatures $T > T_c$; weak temperature dependence $m(T)$ in the temperature range 100–300 K for MP samples; a significant increase in the magnetization of Y-10 sample at low temperatures.

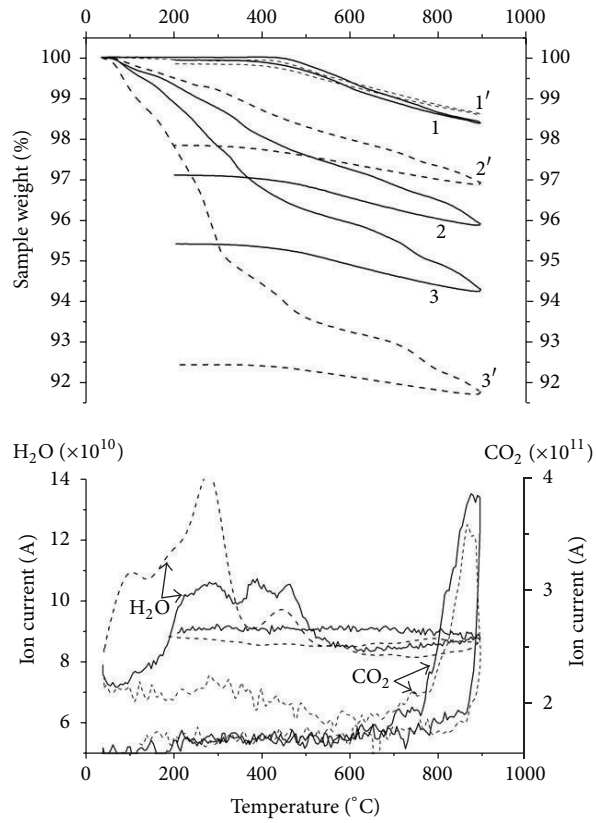

Figure 7: Thermal analysis results for samples: Y-0 (1), N-0 (1′); Y-2 (2), N-2 (2′) and Y-10 (3), N-10 (3′). Mass spectrometry data are related to the samples Y-10 (solid curves) and N-10 (dashed lines).

For comparison, Figure 9 shows the temperature dependence of the FC magnetization in a magnetic field H = 500 Oe for two new samples of Y-123 ($\delta \approx 0.7$). The first sample has been freshly prepared and the other one has been subjected to treatment at 297 ± 1 K for 120 h at absolute humidity of 2.3 κPa. The sample with low oxygen content (and as a consequence with low T_c) has been chosen due to its relatively easy moisture saturation in these conditions without the use of MA (moisture saturation was controlled by the increase in weight, which eventually was ~4 wt.%). One can see that the sample saturated with water has a positive magnetic moment above the temperature T_c and shows an increase in magnetic moment on cooling below this

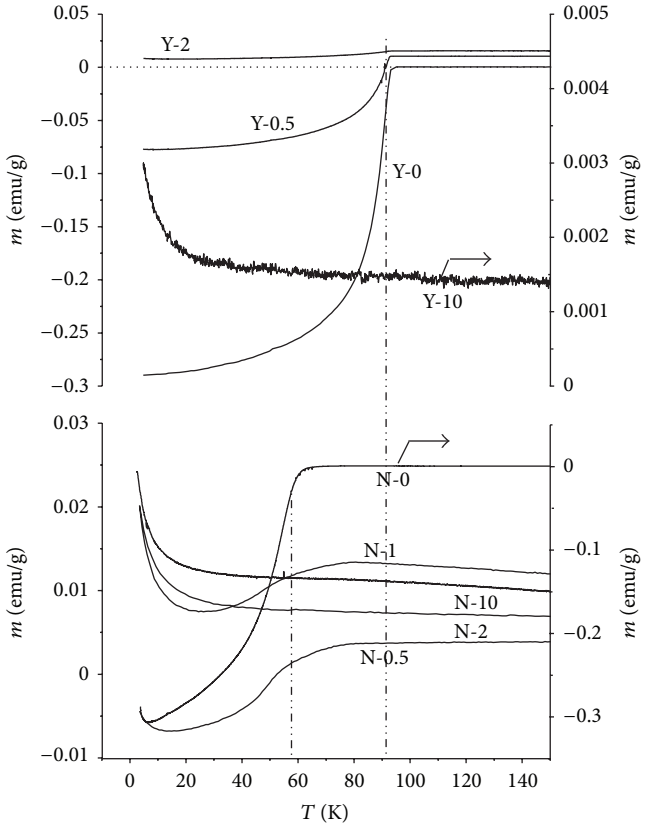

Figure 8: ZFC magnetizations as a function of temperature at $H = 50$ Oe for the initial and mechanically activated samples: $YBa_2Cu_3O_{6+\delta}$ (top); $NdBa_2Cu_3O_{6+\delta}$ (bottom).

temperature similarly to Y-10 sample. Onset temperature of the magnetic anomaly in the hydrated sample is the same as that in the freshly prepared sample. This experiment demonstrates that the presence of water in MP samples has a significant effect on the temperature dependences of the magnetization observed in samples of Y-123 series (see Figure 8).

Temperature dependences of ZFC magnetization of MP samples in Nd-123 series are shown in Figure 8. The superconducting transition temperatures of the samples N-0, N-0.5, and N-1 are independent of milling duration and equal to $T_c \sim 57$ K. Mechanical treatment leads to a substantial change in the magnetization of MP samples throughout the investigated temperature range. MP samples exhibit near-room-temperature hysteretic behavior; that is, ZFC magnetization is more diamagnetic than FC magnetization. It may be due to magnetic particles of mechanoactivated Nd-123 samples or to the presence of impurity phases, whose low content or highly disordered crystal structures do not allow to observe these phases by X-ray diffraction measurements. We also cannot exclude the formation of CuO phase ($T_N \sim 220$ K) at the surface of large $NdBa_2Cu_3O_{6+\delta}$ particles proceeding under mechanical activation. At the same time, a significant increase in the paramagnetic contribution to the magnetization with increasing milling duration is observed.

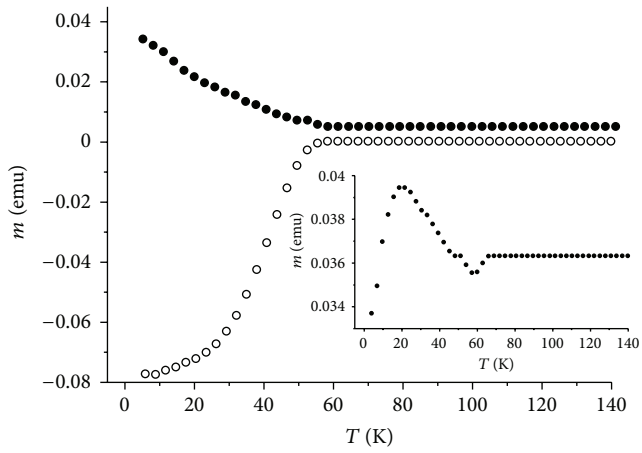

Figure 9: FC magnetizations as a function of temperature of freshly prepared $YBa_2Cu_3O_{6+\delta}$ sample (empty points) and of hydrated sample (black points) at $H = 500$ Oe. Inset: the temperature dependence of magnetization of hydrated sample at $H = 10$ kOe.

A wide transition width around $T_c = 57$ K ($|\Delta T_c \sim 20$ K$|$) in MP samples of Nd-123 series cannot be explained only by the presence of water in the structure. The observed changes indicate that during MA treatment diffusion processes associated with the ordering of the cations Nd^{3+} and Ba^{2+} apparently occur; according to [8–10], that has a significant effect on T_c.

4. Discussion of Results

4.1. Interaction of $YBa_2Cu_3O_{6+\delta}$ and $NdBa_2Cu_3O_{6+\delta}$ with CO_2. From comparison of Figures 4 and 5, it is clear that with increasing duration of MA processing (τ_g) the amount of barium-containing impurities on the surface of Nd-123 samples continuously increases up to $\tau_g = 10$ min, in contrast to the situation for the oxide Y-123, for which initially (up $\tau_g = 0.5$ min) sudden change and subsequent (after $\tau_g = 0.5$ min) almost stagnation in the accumulation of chemical degradation products were observed (see Figures 2 and 3 and data on the impurities in $YBa_2Cu_3O_{6+\delta}$ sample). One can see from Figure 7 that the degree of water saturation (η) of both oxides (this parameter can be traced by sharp descending branch of sample mass change in the temperature range of 30–450°C) obeys similar relationships with increasing τ_g: its growth with increasing MA duration close to proportional for Nd-123 ($\eta \sim \tau_g$), and tendency of η to decrease for Y-123 ($\eta = 1.55 \cdot \tau_g^{0.3}$), which is close to the root dependence, characteristic of reagent diffusion through the reaction products layer.

Taking into account the data in [1], stating the chemical degradation of Y-123 is carried out on the interface between Y-123 and gas phase, and one can explain sharply falling rates of change in concentration of its products, as well as of H_2O dissolved in the oxide; the diffusion path length of H_2O and CO_2 reactants to the location of the reactions (1) and (2) increases with time τ_g. However, the uniformity of the absorption of H_2O and CO_2 gases by MP of Nd-123 testifies

that the thickness of the degraded layer on the surface varies slightly. Apparently, it does not exceed 10 nm, as indicated by a weak but clear signal of the main phase, which appeared in the Ba 4d-spectrum of N-10 sample (see Figure 5). However, it should be noted that Nd-123 MP sample actively enters into chemical reaction with atmospheric CO_2, the gas escapes from the samples quite intensively when heated in the range of 800–900°C (see Figure 7). Therefore, the question of localization place of products of interaction between Nd-123 and atmospheric components arises.

Homogeneous nucleation and growth of interaction products in the volume of $Nd_{1+x}Ba_{2-x}Cu_3O_{6+\delta}$ parent phase may be the answer. This assumption is based on the fact that the products of thermal desorption of N-10 sample (see Figure 7) contain weakly bound form of CO_2 escaping in a wide temperature range of 200–550°C. Obviously, it is a form of gas dissolved in the structure. Since the carbonization energy of Ba^{2+} ions is quite high, homogeneous nucleation of carbonate phase at a certain concentration (≡activity) of CO_2 in the structure, facilitated by the participation of structural defects (whose concentration should be significant in MP samples), seems quite possible.

4.2. Interaction of $YBa_2Cu_3O_{6+\delta}$ and $NdBa_2Cu_3O_{6+\delta}$ with Water. In the Introduction, we have put links to works stating that the crucial feature for the practical application of the superconductor Nd-123 is its high resistance to chemical degradation under moisture. Additional information that expands understanding of this feature has been received in our study. Thus, it is shown (see Figure 7) that a high concentration of water accumulates in MP samples of Nd-123 in dissolved form, but the hydrolysis reaction development is quite limited, as evidenced by the relatively low temperature of H_2O release from this oxide. Moreover, the results of XRD and XPS analyzes have not detected even traces of the ternary compound Nd_2BaCuO_5 in these samples, while it is the compounds R_2BaCuO_5 due their characteristic colours that are indicators of the hydrolysis reaction for the whole family of compounds R-123 [1, 39, 40]. Thus, if the hydrolysis reaction develops (there is a small peak on H_2O desorption curve for sample N-10 at ~455°C that can be attributed to the chemically bound water), then it proceeds through nontraditional mechanism and with low rate.

According to [41], the hydration mechanism for the homologous series of R-123 compounds is in four stages. At the initial stage, water molecules penetrate into the bulk of the crystallites through the structural channels [(1/2) *b* 0], located in interspaces between CuO-chains typical for this type of superconductors. At the next stage, protons, which are located in the oxygen positions of CuO-chains, can be split up of water molecules. This proton transfer is considered to cause an internal (within the $[Cu–O]^+$-system) charge transfer, resulting in formation of molecular oxygen, leaving the structure. At high concentrations of hydroxide ions accumulated in the structure, the chemical decomposition of the initial oxide occurs. Based on the previous scheme, one can understand the reasons for high resistivity of N-123 superconductor to chemical interaction with water.

The authors of [42] discussed the high corrosion resistance of Nd-123 films in the water compared to the film structures of Y-123 and Eu-123, which was attributed to the partial oxygen disorder in the planes of CuO-chains. Such a disorder should occur in Nd-123 due to the presence of some amount of Nd^{3+} ions in the sites nearby to CuO-planes of divalent barium. According to the authors, that should lead to overlapping structural channels for H_2O diffusion and, hence, blocking the hydration process. However, our data on the thermal analysis (see Figure 7) illustrate that the saturation of Nd-123 structure with water during MA treatment proceeds almost as fast as in Y-123 (in the range of 2–10 minutes, even faster). Therefore, the sought cause of the chemical stability of Nd-123 MP cannot be related to problems of H_2O diffusion.

The stage of removing oxygen from the structure is considered [41, 42] to be extremely important for the hydration process of R-123. Thus, the chemical degradation of Y-123 oxide immersed in the water is completely stopped under potential of 0.8 V relative to the standard electrode-saturated sodium calomel [41]. It is expected that the substitution $Nd^{3+} \rightarrow Ba^{2+}$ in Nd-123 in addition to oxygen disordering in the base structural plane should also lead to the strengthening of its bond with the lattice (due to electrostatic effect of highly charged Nd^{3+} ion) [42]. According to the authors [42], this should inhibit the reduction stage of hydration. However, it is important to consider the fact that the structure of MP of Nd-123 contains a large amount of weakly bound CO_2, located near Ba ions (since there is a tendency to the formation of $BaCO_3$), therefore, localized in the channels of the base plane [(1/2) *b* 0], where also there is water. In our opinion, just these CO_2 particles block channels of oxygen desorption, which is the main reason for the high stability of Nd-123 in relation to the hydrolysis reaction.

5. Conclusion

Thus, as a result of mechanical activation treatment, the surface of $YBa_2Cu_3O_{6+\delta}$ is covered by products of hydrolysis and carbonization to a considerable depth. The chemical degradation process proceeds the normal way—through the formation of Y_2BaCuO_5 phase.

Chemical degradation of mechanoactivated $NdBa_2Cu_3O_{6+\delta}$ powders under the impact of CO_2 is not directly connected to hydrolysis process, as occurs in $YBa_2Cu_3O_{6+\delta}$ (see reactions (1) and (2)). Carbonization proceeds homogeneously through the stage of carbon dioxide dissolution in the lattice of $NdBa_2Cu_3O_{6+\delta}$. In its turn, the presence of CO_2 molecules in the structure of mechanoactivated $NdBa_2Cu_3O_{6+\delta}$ powders leads to a radical change in the mechanism of interaction between the superconductor and water. This mechanism eliminates the normal for a homologous series of $RBa_2Cu_3O_{6+\delta}$ the hydrolysis reaction with the formation of characteristic "color" R_2BaCuO_5 phases. The rate of chemical decomposition of mechanically activated $NdBa_2Cu_3O_{6+\delta}$ by the new mechanism (not yet studied) is quite low.

Mechanical treatment affects the temperature dependence of the magnetization of $RBa_2Cu_3O_{6+\delta}$ compounds. There is a significant increase in the paramagnetic and ferromagnetic contributions to the magnetization with increasing milling duration. The latter leads to near-room-temperature hysteretic behavior of $NdBa_2Cu_3O_{6+\delta}$ samples between ZFC and FC regimes. It may be due to magnetic particles of mechanoactivated $NdBa_2Cu_3O_{6+\delta}$ samples or to the presence of impurity phases, whose low content or highly disordered crystal structures do not allow to observe these phases by X-ray diffraction measurements. The mechanical treatment does not have substantial influence on the transition temperatures of superconducting phases T_c in the $RBa_2Cu_3O_{6+\delta}$ compounds, but a wide transition width around T_c indicates that mechanically activated samples contain inhomogeneous superconductor phases with different T_c. The broadening of the superconducting transition in mechanically activated $NdBa_2Cu_3O_{6+\delta}$ samples may be due to redistribution of cations between Nd- and Ba-sublattice.

Finally, we note that the high temperature superconductor $RBa_2Cu_3O_{6+\delta}$, subjected to mechanical activation certainly has no significant advantages over conventional nonmechanoactivated material, but it is obvious that physical-chemical studies of such powders reveal results interesting from the point of view of fundamental science.

Acknowledgment

This work was supported by Russian Foundation for Basic Research (Grant no. 11-03-00317-a).

References

[1] I. E. Graboi, A. R. Kaul', and G. Yu. Metlin, "Advances in science and technology," in *Solid State Chemistry*, pp. 3–142, VINITI AN SSSR, Moscow, Russia, 1989.

[2] S. Anders, M. G. Blamire, F.-Im. Buchholz et al., "European roadmap on superconductive electronics—status and perspectives," *Physica C*, vol. 470, no. 23-24, pp. 2079–2126, 2010.

[3] B. Ruck, B. Oelze, R. Dittmann et al., "Measurement of the dynamic error rate of a high temperature superconductor rapid single flux quantum comparator," *Applied Physics Letters*, vol. 72, no. 18, pp. 2328–2330, 1998.

[4] M. W. Rupich, X. Li, C. Thieme et al., "Advances in second generation high temperature superconducting wire manufacturing and R&D at American superconductor corporation," *Superconductor Science and Technology*, vol. 23, no. 1, Article ID 014015, 2010.

[5] A. Rakitin, M. Kobayashi, and A. P. Litvinchuk, "Superionic behavior of high-temperature superconductors," *Physical Review B*, vol. 55, no. 1, pp. 89–92, 1997.

[6] T. Kagiyama, J. Shimoyama, K. D. Otzschi et al., "Effect of cation composition and oxygen nonstoichiometry on J_c-B properties of Nd123," *Physica C*, vol. 341–348, no. 2, pp. 1445–1446, 2000.

[7] M. Badaye, J. G. Wen, K. Fukushima et al., "Superior properties of $NdBa_2Cu_3O_y$ over $YBa_2Cu_3O_x$ thin films," *Superconductor Science and Technology*, vol. 10, no. 11, pp. 825–830, 1997.

[8] C. Cantoni, D. P. Norton, D. M. Kroeger et al., "Phase stability for the in situ growth of $Nd_{1+x}Ba_{2-x}Cu_3O_y$ films using pulsed-laser deposition," *Applied Physics Letters*, vol. 74, no. 1, pp. 96–98, 1999.

[9] E. A. Goodilin, N. N. Oleynikov, E. V. Antipov et al., "Phase stability for the in situ growth of $Nd_{1+x}Ba_{2-x}Cu_3O_y$ films using pulsed-laser deposition," *Physica C*, vol. 272, 6578 pages, 1996.

[10] E. Guilmeau, F. Giovannelli, I. Monot-Laffez, S. Marinel, J. Provost, and G. Desgardin, "Top seeding melt texture growth of NdBaCuO pellets in air," *The European Physical Journal*, vol. 13, no. 3, pp. 157–160, 2001.

[11] A. I. Ancharov, T. F. Grigor'eva, T. Yu. Kiseleva, A. A. Novakova et al., in *Mechanocomposites-Precursorsfor the Creation of Materials with New Properties*, O. I. Lomovskii, Ed., p. 424, Izd-vo. SO RAN, Novosibirsk, Russia, 2010.

[12] A. Hamrita, F. Ben Azzouz, A. Madani, and M. Ben Salem, "Magnetoresistivity and microstructure of $YBa_2Cu_3O_y$ prepared using planetary ball milling," *Physica C*, vol. 472, no. 1, pp. 34–38, 2012.

[13] R. P. Vasquez, "Intrinsic photoemission signals, surface preparation, and surface stability of high temperature superconductors," *Journal of Electron Spectroscopy and Related Phenomena*, vol. 66, no. 3-4, pp. 209–222, 1994.

[14] S. S. Gorelik, L. N. Rastorguev, and A. Yu. Skakov, in *RentgenographIcheskII I ElektronographIcheskII AnalIz*, p. 368, Izd-vo Metallurgia, Moscow, Russia, 1970.

[15] M. V. Reshetniak and O. V. Sobol, Program for diffraction analysis "New_Profile"(Last update 10. 02. 2007) Version 3. 4. 400 (Freeware) WIN9x/ME/NT/2K/XP Copyright (c) 1992-2007 ReMax SoftWare 2000.

[16] M. Wegmann, L. Watson, and A. Hendry, "XPS analysis of submicrometer barium titanate powder," *Journal of the American Ceramic Society*, vol. 87, no. 3, pp. 371–377, 2004.

[17] A. B. Christie, J. Lee, I. Sutherland, and J. M. Walls, "An XPS study of ion-induced compositional changes with group II and group IV compounds," *Applications of Surface Science*, vol. 15, no. 1–4, pp. 224–237, 1983.

[18] U. A. Joshi, S. Yoon, S. Balk, and J. S. Lee, "Surfactant-free hydrothermal synthesis of highly tetragonal barium titanate nanowires: a structural investigation," *Journal of Physical Chemistry B*, vol. 110, no. 25, pp. 12249–12256, 2006.

[19] R. Caracciolo, "Chemical characterization techniques for thin films," in *Ceramic Films and Coatings*, J. B. Wachtman and R. A. Haber, Eds., p. 376, New Jersey, NJ, USA, 1992.

[20] I. N. Shabanova, Y. A. Naimushina, and N. S. Terebova, "Composition and temperature dependence of a Y-Ba-Cu-O HTSC electronic structure," *Superconductor Science and Technology*, vol. 15, no. 7, pp. 1030–1033, 2002.

[21] J. Beyer, T. Schurig, S. Menkel, Z. Quan, and H. Koch, "XPS investigation of the surface composition of sputtered YBCO thin films," *Physica C*, vol. 246, no. 1-2, pp. 156–162, 1995.

[22] C. C. Chang, M. S. Hegde, X. D. Wu et al., "Surface layers on superconducting Y-Ba-Cu-O films studied with x-ray photoelectron spectroscopy," *Applied Physics Letters*, vol. 55, no. 16, pp. 1680–1682, 1989.

[23] X. D. Wu, A. Inam, M. S. Hegde et al., "Crystalline perfection of as-deposited high-Tc superconducting thin-film surfaces: ion channeling and x-ray photoelectron spectroscopy study," *Physical Review B*, vol. 38, no. 13, pp. 9307–9310, 1988.

[24] P. Rajasekar, P. Chakraborty, S. K. Bandyopadhyay, P. Barat, and P. Sen, "X-ray photoelectron spectroscopy study of oxygen and

argon annealed $YBa_2 2Cu_3O_{7-\delta}$," *Modern Physics Letters B*, vol. 12, no. 6-7, pp. 239–245, 1998.

[25] J. Halbritter, P. Walk, H. J. Mathes, B. Haeuser, and H. Rogalla, "ARXPS-studies of ĉ-axis textured $YBa_2Cu_3O_x$-films," *Physica C*, vol. 153–155, no. 1, pp. 127–128, 1988.

[26] T. J. Šarapatka and P. Mikušík, "XPS study of Pb/YBaCuO thin-film tunnel contact," *Applied Surface Science*, vol. 68, no. 1, pp. 35–40, 1993.

[27] J. A. T. Verhoeven and H. Van Doveren, "An XPS investigation of the interaction of CH_4, C_2H_2, C_2H_4 and C_2H_6 with a barium surface," *Surface Science*, vol. 123, no. 2-3, pp. 369–383, 1982.

[28] C. D. Wagner, W. M. Riggs, L. E. Davis, J. F. Moulder, and G. E. Mullenberg, *Handbook of X-Ray Photoelectron Spectroscopy*, Perkin-Elmer Corp, Eden Prairie, Minn, USA, 1979.

[29] M. C. Biesinger, L. W. M. Lau, A. R. Gerson, and R. S. C. Smart, "Resolving surface chemical states in XPS analysis of first row transition metals, oxides and hydroxides: Sc, Ti, V, Cu and Zn," *Applied Surface Science*, vol. 257, no. 3, pp. 887–898, 2010.

[30] X. Y. Fan, Z. G. Wu, P. X. Yan et al., "Fabrication of well-ordered CuO nanowire arrays by direct oxidation of sputter-deposited Cu_3N film," *Materials Letters*, vol. 62, no. 12-13, pp. 1805–1808, 2008.

[31] S. J. Kerber, J. J. Bruckner, K. Wozniak, S. Seal, S. Hardcastle, and T. L. Barr, "Nature of hydrogen in x-ray photoelectron spectroscopy: general patterns from hydroxides to hydrogen bonding," *Journal of Vacuum Science and Technology A*, vol. 14, no. 3, pp. 1314–1320, 1996.

[32] G. Moretti, G. Fierro, M. Lo Jacono, and P. Porta, "Characterization of CuO-ZnO catalysts by X-ray photoelectron spectroscopy: precursors, calcined and reduced samples," *Surface and Interface Analysis*, vol. 14, no. 6-7, pp. 325–336, 1989.

[33] H. Van Doveren and J. A. T. H. Verhoeven, "XPS spectra of Ca, Sr, Ba and their oxides," *Journal of Electron Spectroscopy and Related Phenomena*, vol. 21, no. 3, pp. 265–273, 1980.

[34] B. V. Crist, *Handbooks of Monochromatic XPS Spectra. Volume 2—Commercially pure binary oxides*, XPS International LLC, Leona, Tex, USA, 2005.

[35] D. D. Sarma and C. N. R. Rao, "XPES studies of oxides of second- and third-row transition metals including rare earths," *Journal of Electron Spectroscopy and Related Phenomena*, vol. 20, no. 1, pp. 25–45, 1980.

[36] V. I. Nefedov and A. N. Sokolov, "Degradatzia visokotemperaturnich sverchprovodnikov pri khimicheskich vozdeistviach," *Zhurnal Neorganicheskoi Khimii*, vol. 34, no. 11, pp. 2723–2739, 1989.

[37] Y. Uwamino, T. Ishizuka, and H. Yamatera, "X-ray photoelectron spectroscopy of rare-earth compounds," *Journal of Electron Spectroscopy and Related Phenomena*, vol. 34, no. 1, pp. 67–78, 1984.

[38] M. P. Seah and W. A. Dench, "Quantitative electron spectroscopy of surfaces: a standard data base for electron inelastic mean free paths in solids," *Surface and Interface Analysis*, vol. 1, no. 1, pp. 2–11, 1979.

[39] C. H. Lin, H. C. I. Kao, and C. M. Wang, "Kinetics and stability of $R(Ba_{1.5}Sr_{0.5})Cu_3O_y$ (R = La, Nd, Sm, Eu, Gd, Dy, Ho) superconductors in water," *Materials Chemistry and Physics*, vol. 82, no. 2, pp. 435–439, 2003.

[40] A. G. Knizhnik, R. A. Stukan, and G. O. Eremenko, "Study the interaction between europium HTSC of 123 type and water," *Sverkhprovodimost*, vol. 4, no. 1, pp. 177–182, 1991 (Russian).

[41] J. Zhou, R. K. Lo, J. T. McDevitt et al., "Development of a reliable materials base for superconducting electronics," *Journal of Materials Research*, vol. 12, no. 11, pp. 2958–2975, 1997.

[42] S. B. Schougaard, M. F. Ali, and J. T. McDevitt, "Evidence for high stability against water corrosion of $NdBa_2Cu_3O_{7\pm\delta}$ relative to $YBa_2Cu_3OO_{7-\delta}$ and $EuBa_2Cu_3OO_{7-\delta}$," *Applied Physics Letters*, vol. 84, no. 7, pp. 1144–1146, 2004.